

ISATIN/THIOSEMICARBAZONE HYBRIDS: FACILE SYNTHESIS, AND THEIR EVALUATION AS ANTI-PROLIFERATIVE AGENTS AND METABOLIC ENZYME INHIBITORS

Hasan Yakan¹, Mohammed Azam^{2*}, Sevgi Kansız³, Halit Muğlu⁴, Mustafa Ergül⁵, Parham Taslimi⁶, Ümit M. Koçyiğit^{5*}, Muhammet Karaman⁷, Saud I. Al-Resayes² and Kim Min⁸

¹Department of Science and Mathematics Education, Ondokuz Mayıs University, Samsun, Turkey

²Department of Chemistry, College of Science, King Saud University, P.O. Box 2455, Riyadh 11451, Saudi Arabia

³Samsun University, Faculty of Engineering, Department of Fundamental Sciences, Samsun, 55420, Turkey

⁴Department of Chemistry, Kastamonu University, Kastamonu, Turkey

⁵Department of Basic Pharmaceutical Sciences, Sivas Cumhuriyet University, Sivas, Turkey

⁶Department of Biotechnology, Faculty of Science, Bartın University, Bartın, Turkey

⁷Department of Molecular Biology and Genetics, Kilis 7 Aralık University, Kilis, Turkey

⁸Department of Safety Engineering, Dongguk University, 123 Dongdae-ro, Gyeongju 780714, Gyeongbuk, South Korea

(Received February 22, 2023; Revised June 10, 2023; Accepted June 15, 2023)

ABSTRACT. We are reporting a novel series of thiosemicarbazone derivatives derived from isatin (**1-6**), structural determination, and investigation of the inhibitory properties against proliferative, carbonic anhydrase, and cholinesterase enzymes. The anti-proliferative effects of the compounds were measured by XTT assay against MCF-7 and MDA-MB-231 cancerous cell lines. Compound **3** showed significant cytotoxic effects on both MCF-7 and MDA-MB-231 cell lines, with IC₅₀ values of 8.19 μ M and 23.41 μ M, respectively. In addition, the compounds (**1-6**) inhibited the hCA I and II, their K_i values 2.01 \pm 0.35 – 21.55 \pm 2.56 and 1.24 \pm 0.33 – 25.03 \pm 5.48 μ M, respectively. AChE was also successfully inhibited by these compounds (**1-6**), with K_i values ranging from 40.37 \pm 8.23 to 125.43 \pm 24.93 μ M. The best K_i values for **3**, **6**, and **4** for α -glucosidase were 564.35 \pm 72.06, 594.38 \pm 52.04, and 683.437 \pm 66.58 μ M, respectively. Binding affinities were determined to be -6.697 kcal/mol, -8.251 kcal/mol, -9.932 kcal/mol, and -4.946 kcal/mol for hCA I, hCA II, AChE, and α -glucosidase enzymes, respectively. These findings reveal that the formed compounds containing isatin moieties were crucial in the enzyme inhibition.

KEY WORDS: Isatin, Thiosemicarbazone, Anti-proliferative activity, Enzyme inhibition, Molecular docking

INTRODUCTION

Cancer, one of the worst diseases in the world, is responsible for the deaths of an increasing number of people. Therefore, the development of novel, safe, and selective anti-cancer compounds has become a major goal for medicinal chemistry researchers as most of the existing anti-cancer drugs are highly hazardous [1-3]. Alzheimer's is an extremely tough disease to manage, especially for the elderly people, and it has a significant impact on quality of life of people. The illness might be categorized as cognitive deterioration with strong executive function difficulties. In addition, this disease is a progressive brain disorder that gradually robs people of their capability for reasoning, memory, and doing basic tasks [4-6]. Although the exact cause of this disease is still unknown, however, several factors, including acetylcholine (ACh) deficiency, excessive amyloid-beta (β -amyloid) peptide development, neurofibrillary node (NFT) formation,

*Corresponding author. E-mail: azam_res@yahoo.com, ukoeyigit@cumhuriyet.edu.tr

This work is licensed under the Creative Commons Attribution 4.0 International License

metal homeostasis disruption, and reactive oxygen species formation, are important in brain disruption [7-9].

Alpha-glucosidase is the principal target of type 2 diabetes treatment and medication research. The three most clinically effective medications for type 2 diabetes are alpha-glucosidase inhibitors that work by lowering PPGFF (Acarbose, Miglitol, and Voglibose) (post-prandial hyperglycemia). Acetylcholine (ACh) breakdown into choline and acetic acid, a critical process for cholinergic neurotransmission repair, is catalyzed by a class of enzymes known as cholinesterases (ChE). The Food and Drug Administration has only approved medicines like tacrine, donepezil, and rivastigmine for the treatment of Alzheimer's disease, even though there are numerous ongoing research projects in this area (FDA) [10-12].

Over the years, researchers have also developed new cholinesterase inhibitor medications using various isatin derivatives [13]. Various physiological and pathological metabolic pathways involve members of the isozyme family of carbonic anhydrase. In order to manage and transport different CO₂-bound chemical forms via biological membranes such intracellular and extracellular regions [14-17], these enzymes catalyze the basic reaction of reversible hydration of carbon dioxide to bicarbonate and protons.

Isatin, a crucial class of organic compounds found in both plant and human tissue, have emerged as a potentially fruitful nucleus in recent years, sparking an increase in interest in pharmaceutical chemistry and medication development. Furthermore, isatin exhibit a variety of biological activities, including anti-cancer [18, 19], antioxidant [20, 21], anti-HIV reverse transcriptase inhibition [22], anti-fungal [23], and anti-bacterial [24]. Studies have also shown that the isatin ring can be exploited as a significant component of anticancer hybrid compounds [25, 26]. Additionally, it has been revealed that several isatin-derived carbonate anhydrase inhibitors exist in literature [27, 28].

Thiosemicarbazones, as another important family of heterochemistry, share many of the same biological and therapeutic properties as other heterocycles [29-31]. It may be possible to produce novel therapeutic compounds using molecular hybridization based on the activity of certain subunits in the molecular skeleton of two or more physiologically active derivatives. In recent years, a lot of curiosity in the development of hybrid derivatives that may simultaneously bind to multiple biological targets has grown [32, 33]. It, therefore, is essential to treat disease with hybrid molecules in order to reduce the likelihood of adverse drug reactions and to keep drug resistance to a minimum.

Therefore, considering the wide significance of thiosemicarbazones, we investigated novel compounds to interpret thiosemicarbazones including isatin groups to explore anticancer, enzyme inhibitory activities, and theoretical features. However, there are not many studies on isatin derivatives utilised as carbonic anhydrase inhibitors and anticancer medications in the literature [23, 34]. This is the first study of thiosemicarbazone compounds derived from isatin as possible anti-cancer medicines and carbonic anhydrase enzyme inhibitors, and these features of the produced thiosemicarbazone have not been reported in the literature (Figure 1). In order to combat cancer and inhibit enzymes, we have therefore designed and produced thiosemicarbazone compounds derived from isatin, and studied how they affect the inhibition of hCA I and II isoforms, and assessed their anti-cancer potential. In addition, we also investigate the interaction of the examined compounds with the aforementioned metabolic enzymes through molecular docking studies.

EXPERIMENTAL

Instruments and chemicals

Both reagents and solvents were purchased and used without further purification from Acros Organics, Sigma-Aldrich, or Merck Chemical Company. They were solvents of a spectroscopic standard. To measure melting points, a Stuart Melting Point 30 apparatus was used and

uncorrected. The basic analysis was conducted on a Eurovector EA3000-Single. For infrared spectrum recording, a Bruker Alpha Fourier transform IR (FT-IR) spectrometer was used. ^1H and ^{13}C NMR spectra were taken on a Bruker Avance DPX-400 spectrophotometer (400 MHz) in $\text{DMSO-}d_6$.

Synthesis of the compounds (1-6)

All compounds were obtained using the reported procedure with slight modifications in good yields (65-92%) [29]. However, compound **6** was prepared following the method described in literature [35].

Compound 1. Orange solid, 67% yield, Mp; 270-271 °C. IR (cm^{-1}): 3332, 3304, 3238 (NH^1 , NH^2 , NH^3), 3062 (ArC-H), 2964-2833 (Aliph C-H), 1694 (C=O), 1548 (C=N), 1435 (C=S), 1293 (C-N), 1132 (C-O). ^1H NMR (400 MHz, DMSO) δ 12.59 (s, NH^1), 11.03 (s, NH^2), 9.27-9.26 (q, NH^3), 7.27-7.26 (d, Ar H1, 1H), 6.96-6.93 (dd, Ar H2, 1H), 6.86-6.84 (d, Ar H3, 1H), 3.77 (s, OCH_3), 3.10-3.09 (d, CH_3). ^{13}C NMR (101 MHz, DMSO) δ 178.2 (C=S), 163.2 (C=O), 155.8 (C1), 136.43 (C=N), 132.36, 121.30, 117.68, 112.30, 106.42, 56.09 (OCH_3), 31.80 (CH_3). Elemental analysis calcd for $\text{C}_{11}\text{H}_{12}\text{N}_4\text{O}_2\text{S}$: C, 49.99; H, 4.58; N, 21.20. Found: C, 49.77; H, 4.61; N, 21.27.

Compound 2. Dark yellow solid, 65% yield, Mp; 247-248 °C. IR (cm^{-1}): 3312, 3256 (NH^1 , NH^2 , NH^3), 3001 (ArC-H), 2940-2834 (Aliph C-H), 1684 (C=O), 1527 (C=N), 1431 (C=S), 1289 (C-N), 1139 (C-O). ^1H NMR (400 MHz, DMSO) δ 12.57 (s, NH^1), 11.02 (s, NH^2), 9.30-9.27 (t, NH^3), 7.28-7.27 (d, Ar H1, 1H), 6.95-6.92 (dd, Ar H2, 1H), 6.85-6.83 (d, Ar H3, 1H), 3.77 (s, OCH_3), 3.69-3.62 (p, CH_2), 1.22-1.18 (t, CH_3). ^{13}C NMR (101 MHz, DMSO) δ 177.2 (C=S), 163.2 (C=O), 155.8 (C1), 136.4 (C=N), 132.4, 121.3, 117.6, 112.2, 106.6, 56.1 (OCH_3), 39.5 (CH_2), 14.5 (CH_3). Elemental analysis calcd for $\text{C}_{12}\text{H}_{14}\text{N}_4\text{O}_2\text{S}$: C, 51.78; H, 5.07; N, 20.13. Found: C, 51.64; H, 5.11; N, 20.14.

Compound 3. Yellow solid, 81% yield, Mp; 201-202 °C. IR (cm^{-1}): 3282, 3235 (NH^1 , NH^2 , NH^3), 3012 (ArC-H), 2932-2830 (Aliph C-H), 1692 (C=O), 1518 (C=N), 1433 (C=S), 1317 (C-N), 1128 (C-O). ^1H NMR (400 MHz, DMSO) δ 12.63 (s, NH^1), 11.02 (s, NH^2), 9.46-9.43 (t, NH^3), 7.28-7.27 (d, Ar H1, 1H), 6.94-6.91 (dd, Ar H2, 1H), 6.84-6.82 (d, Ar H3, 1H), 5.97-5.90 (m, $-\text{CH}=\text{C}$), 5.22-5.14 (dd, $=\text{CH}_2$), 4.28-4.27 (d, $-\text{CH}_2$), 3.76 (s, OCH_3). ^{13}C NMR (101 MHz, DMSO) δ 177.8 (C=S), 163.2 (C=O), 155.8 (C1), 136.5 (C=N), 132.6, 121.3, 117.7, 112.3, 106.6, 134.4 ($\text{CH}=\text{C}$), 116.7 ($=\text{CH}_2$), 46.8 (CH_2), 56.1 (OCH_3). Elemental analysis calcd for $\text{C}_{13}\text{H}_{14}\text{N}_4\text{O}_2\text{S}$: C, 53.78; H, 4.86; N, 19.30. Found: C, 53.64; H, 4.81; N, 19.24.

Compound 4. Dark red solid, 85% yield, Mp; 198-199 °C. IR (cm^{-1}): 3224 (NH^1 , NH^2 , NH^3), 3052 (ArC-H), 2982-2870 (Aliph C-H), 1691 (C=O), 1598 (C=N), 1421 (C=S), 1266 (C-N), 1146 (C-O). ^1H NMR (400 MHz, DMSO) δ 12.80 (s, NH^1), 11.07 (s, NH^2), 10.75 (s, NH^3), 7.43-7.42 (d, Ar H6, 1H), 7.36-7.32 (t, Ar H7, 1H), 7.29-7.28 (d, Ar H1, 1H), 7.23-7.21 (d, Ar H8, 1H), 6.97-6.94 (dd, Ar H2, 1H), 6.88-6.87 (d, Ar H4, 1H), 6.86-6.85 (d, Ar H3, 1H), 3.78 (s, Ar- OCH_3), 3.77 (s, ist- OCH_3). ^{13}C NMR (101 MHz, DMSO) δ 176.6 (C=S), 163.3 (C=O), 159.7 (C12), 155.8 (C1), 139.9 (C10), 136.7 (C=N), 133.0, 129.6, 121.2, 118.2, 117.9, 112.3, 112.2, 111.8, 107.2, 56.2 (ist- OCH_3), 55.7 (Ar- OCH_3). Elemental analysis calcd for $\text{C}_{17}\text{H}_{16}\text{N}_4\text{O}_3\text{S}$: C, 57.29; H, 4.53; N, 15.72. Found: C, 57.21; H, 4.49; N, 15.65.

Compound 5. Yellow solid, 78% yield, Mp; 238-239 °C. IR (cm^{-1}): 3350, 3327, 3220 (NH^1 , NH^2 , NH^3), 3100 (ArC-H), 1690 (C=O), 1592 (C=N), 1432 (C=S), 1315 (C-N), 1171 (Ar-F), 967 (Ar-Cl). ^1H NMR (400 MHz, DMSO) δ 12.69 (s, NH^1), 11.23 (s, NH^2), 10.83 (s, NH^3), 7.74 (s, Ar H1, 1H), 7.62-7.57 (m, Ar H2-H3, 2H), 7.44-7.40 (t, Ar H6, 1H), 7.32-7.29 (m, Ar H4, 1H), 7.20-

7.15 (td, Ar H7, 1H), 6.92-6.88 (dd, Ar H8, 1H). ¹³C NMR (101 MHz, DMSO) δ 176.8 (C=S), 163.32, 163.31 (C1), 159.9 (C=O), 157.6 (C12), 142.9 (C=N), 140.3, 139.40, 139.38 (C4), 133.0, 130.6, 126.5, 125.5, 124.5 (C3), 121.7, 118.48, 118.24 (C5), 112.81, 112.73 (C2), 109.01, 108.76 (C6). Elemental analysis calcd for C₁₅H₁₀ClFN₄OS: C, 51.66; H, 2.89; N, 16.06. Found: C, 51.54; H, 2.86; N, 16.02.

Compound 6. Light red solid, 92% yield, Mp; 253-254°C. IR (cm⁻¹): 3308, 3205 (NH¹, NH², NH³), 3043 (ArC-H), 1689 (C=O), 1548 (C=N), 1457 (C=S), 1296 (C-N), 1126 (Ar-F), 949 (Ar-Cl). ¹H NMR (400 MHz, DMSO) δ 12.67 (s, NH¹), 11.36 (s, NH²), 10.80 (s, NH³), 7.81 (d, Ar H1, 1H), 7.51-7.47 (t, Ar H6 1H), 7.43-7.40 (dd, Ar H5, H8, 2H), 7.39-7.34 (dd, Ar H2, 1H), 7.31-7.27 (t, Ar H7, 1H), 6.98-6.95 (d, Ar H3, 1H). ¹³C NMR (101 MHz, DMSO) δ 178.5 (C=S), 163.3, 163.1 (C11), 162.9 (C=O), 156.6 (C1), 141.8 (C=N), 127.0 (C2), 122.3 (C3), 130.7 (C4), 121.4 (C5), 124.9 (C6), 116.6, 116.4 (C10), 113.1, 113.0 (C12), 129.7, 129.6 (C13), 126.8, 126.7 (C14), 131.9, 131.2 (C15). Elemental analysis calcd for C₁₅H₁₀ClFN₄OS: C, 51.66; H, 2.89; N, 16.06. Found: C, 51.59; H, 2.91; N, 15.99.

Enzyme studies

The inhibitory effect of these compounds on the function of the alpha-glycosidase enzyme was assessed using the substrate *p*-nitrophenyl-D-glycopyranoside (*p*-NPG) by Tao *et al.* [36]. First, a phosphate buffer of 200 μL was combined with a phosphate buffer of 40 μL of homogenate (0.15 U/mL, pH 4.7). Furthermore, 50 μL of *p*-NPG was applied to the phosphate buffer after preincubation (5 mM, pH 7.4) and incubated again at 30 °C. According to previous studies, absorbances at 405 nm have been measured spectrophotometrically [8, 17]. The inhibitory effects of thiosemicarbazone derivatives including isatin (**1-6**) on both hCA (I, II) isozymes were represented by Verpoorte *et al.* [37] and spectrophotometrically reported at 348 nm according to the esterase assay using *p*-nitrophenyl acetate (*p*-NPA) substrate. Also, according to the Ellman *et al.* procedure, the inhibitory effects of AChE were identified [38]. They were spectrophotometrically recorded at 412 nm using acetylthiocyanine iodide and in accordance with earlier works, were also recorded as enzymatic reaction substrates [39]. To test AChE operation, 5,5'-dithiobis (2-nitrobenzoic acid) (Ellman reagent, DTNB) was also used.

Cell culture

The human breast cancer cell lines MCF-7 (HTB-22) and MDA-MB-231 (HTB-26) were obtained from the American Type Culture Collection. They were cultured in Dulbecco's modified Eagle's medium (DMEM; Thermo Fisher Scientific) supplemented with 10% fetal bovine serum (Sigma-Aldrich) and 1% penicillin/streptomycin (Sigma-Aldrich). The cells were maintained at 37 °C in a humidified atmosphere containing 5% CO₂. To prepare the compounds for experimentation, they were dissolved in DMSO, and 10 mM stock solutions were created. Prior to application, the stock solutions were diluted with DMEM to ensure that the final concentration of DMSO did not exceed 0.5%.

Molecular docking studies

Crystal structures of hCA I (PDB ID: 4WR7), hCA II (PDB ID: 5AML), AChE (PDB ID: 4M0E), and α-glucosidase (PDB ID: 3A4A) enzymes were obtained from RCSB Protein Data Bank. In silico studies were performed according to the method described in previous studies [17] using Small Drug Discovery Suit (Schrödinger, LLC, 2017). The structures were chosen due to their high resolution and co-crystallized ligand. All compounds were created and prepared with the Ligprep module. Then, the drug-likeness properties of the inhibitors were calculated with the Qikprop module [40]. The structures were made ready for the docking process by preparing with

the Protein preparation wizard module. Binding sites of enzymes were predicted using the Sitemap module. The molecular docking studies of the most effective inhibitors were performed with an induced-fit docking module [40].

Cell viability assay

The cytotoxicity of the synthesized compounds was assessed using the 2,3-bis-(2-methoxy-4-nitro-5-sulfophenyl)-2Htetrazolium-5-carboxanilide (XTT) cell viability assay provided by Roche Diagnostic. The cells were seeded in 96-well plates at a density of 1×10^4 cells per well and allowed to attach overnight. Afterward, the cells were treated with various concentrations of the compounds (5, 10, 20, 40, and 80 μM) for a duration of 48 hours. Following the incubation period, the DMEM medium was aspirated, and the wells were washed with phosphate-buffered saline. Next, 50 μL of XTT labeling solution was added to each well, and the plates were incubated for 4 hours. The absorbances were then measured at 450 nm using a microplate reader from Thermo Fisher Scientific. All experiments were performed in triplicate, and the cell viability was determined by calculating the percentage of viable cells compared to the control cells. To determine the half-maximal inhibitory concentration (IC_{50}) values of the compounds within the cells, the data obtained from the experiments were analyzed using Graph Prism 7 software by GraphPad Software, Inc.

RESULTS AND DISCUSSION

Synthesis and characterization

Figure 1 shows the synthetic route of thiosemicarbazone derivatives. First, hydrazine monohydrate was treated with isothiocyanates in the presence of ethanol in an ice bath. Second, products were formed by reacting formed thiosemicarbazides with 5-substituted isatin in the presence of ethanol and one drop of HCl under reflux.

The FTIR spectra did not reveal stretching vibrations due to ($-\text{NH}_2$) at $3450\text{--}3225\text{ cm}^{-1}$. Instead, additional stretching bands were seen at $1598\text{--}1527\text{ cm}^{-1}$ ascribed to $-\text{C}=\text{N}$ vibrations. These observations turned out as expected. The $=\text{N}\text{--}\text{NH}$ and $-\text{NH}$ stretching vibrations of the thiosemicarbazide region were observed at 3304 and 3238 cm^{-1} , respectively, for compound **1**, while the $-\text{NH}$ stretching vibration of the isatin ring was observed at 3332 cm^{-1} . The $-\text{C}=\text{O}$ stretching vibration was observed at 1694 cm^{-1} whereas $\text{C}=\text{N}$ stretching vibration was observed at 1548 cm^{-1} . In addition, the vibrations due to $-\text{C}=\text{S}$ band was observed at 1435 cm^{-1} , while the $-\text{C}\text{--}\text{N}$ stretching vibration appeared at 1293 cm^{-1} . The $-\text{C}\text{--}\text{O}$ stretching vibration was seen at 1132 cm^{-1} . These values have provided considerable evidence for the formation of the compounds. These findings are consistent with previously reported values for related compounds [29, 41, 42].

The ^1H and ^{13}C NMR spectra of the compounds in $\text{DMSO-}d_6$ were detected. In compound **1**, while the $-\text{NH}$ (N^1) peak of isatin was revealed at 12.59 ppm as a singlet, the $-\text{NH}$ (N^2) signal of thiosemicarbazone was shown as a singlet at 11.03 ppm . But, the $-\text{NH}$ (N^3) proton coupled to the CH_3 ($-\text{R}_1$) group was resonated as quartet at $9.27\text{--}9.26$ ($J = 4.5\text{ Hz}$) ppm. The methyl group ($-\text{CH}_3$) proton coupled to the $-\text{NH}$ (N^3) proton was detected at $3.10\text{--}3.09$ ($J = 4.6\text{ Hz}$) ppm, as a doublet. The isatin proton signals ($\text{H}_1\text{--}\text{H}_2\text{--}\text{H}_3$) were observed at $7.27\text{--}6.84\text{ ppm}$. The H_1 proton coupled to the H_2 proton was shown at $7.27\text{--}7.26$ ($J = 2.5\text{ Hz}$) ppm, as a doublet peak. The H_2 proton coupled to the H_3 and H_1 proton was observed as a doublet of doublets peaks at $6.96\text{--}6.93$ ($J = 8.5, 2.4\text{ Hz}$) ppm. The H_3 proton coupled to the H_2 proton was observed with doublet peaks at $6.86\text{--}6.84$ ($J = 8.5\text{ Hz}$) ppm. The proton signal of the methoxy group ($-\text{OCH}_3$) was observed at 3.77 ppm as a singlet. Based on these observations, our findings are consistent with the previously published data [41, 42].

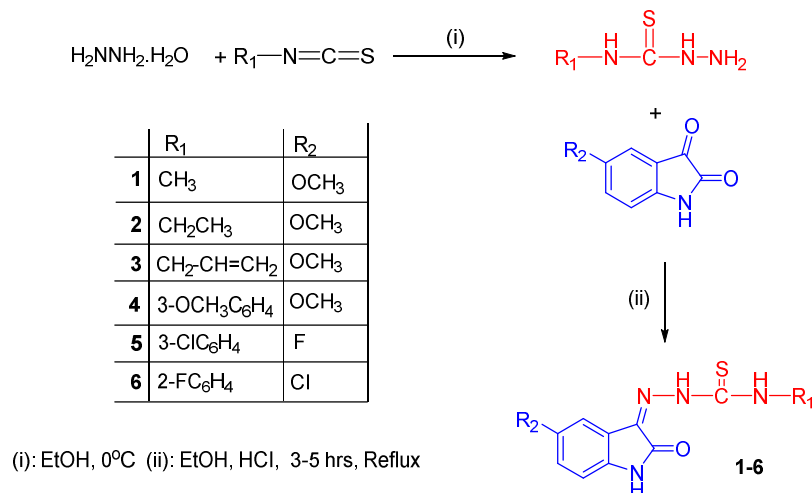


Figure 1. The synthesis of thiosemicarbazone derivatives with isatin.

The ¹³C NMR spectrum of compound **1** revealed 11 different resonances consistent with the targeted product. In compound **1**, thiosemicarbazide' -C=S signal was observed at 178.2 ppm. The -C=N and -C=O substantial specific peaks of the isatin region were detected at 136.4 and 163.2 ppm, respectively. The carbon atom peaks (C1-C6) of the isatin ring were detected at 155.8, 112.3, 121.3, 132.4, 117.7, and 106.4 ppm, respectively. The C1 carbon atom shifted down-field (high value, δ) owing to the presence of the methoxy (-OCH₃) group. The carbon atom of the methoxy was detected at 56.1 ppm. The carbon atom of the methyl group (C10, -CH₃) was detected at 31.8 ppm. The aromatic carbon atoms (C10-C15) of the phenyl ring were observed at between 157.6 and 121.7 ppm for compound **5**. The C12 (157.6 ppm) carbon atom was shifted down-field (high value, δ) because of the presence of the Cl (chlorine) atom. Furthermore, the C atoms (for C1-C6) were also split into doublets owing to interacting with the atomic nucleus of F for compound **5**. The C1 (163.32 and 163.31 ppm) carbon atom was shifted down-field (high value, δ) because of the presence of the F (fluorine) atom.

Anti-proliferative activity

The XTT cell viability assay was used to test the anti-proliferative activity of the compounds under study against human breast cancer cells MCF-7 and MDA-MB-231. Although most of the compounds has weaker anti-proliferative effects on MDA-MB-231 cells, they showed considerable anti-proliferative effects on MCF-7 cells (Figure 2). In addition, compound **3** showed significant cytotoxicity to MCF-7 and MDA-MB-231 cell lines than other compounds.

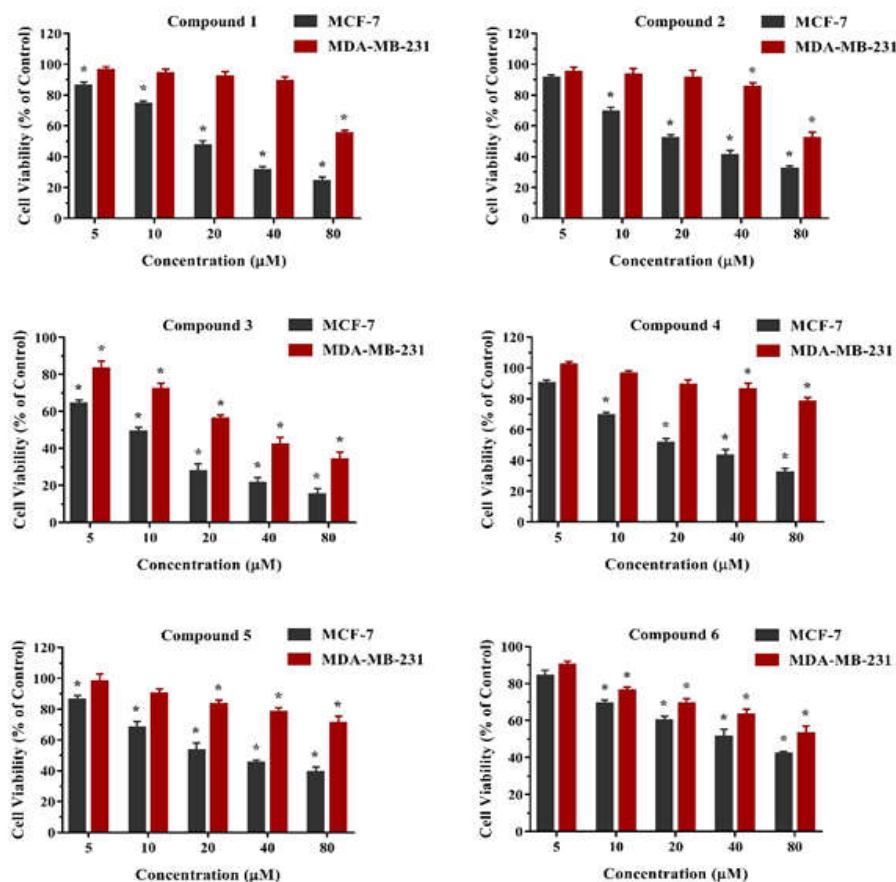


Figure 2. The compound has anti-proliferative activity on MCF-7 and MDA-MB-231 cell lines. The cells were exposed to different concentrations (5-80 µM) of compounds for 48 h. XTT analysis was then used to assess cell viability. All data are repeated three times with mean \pm SD. The difference from untreated control cells was identified as * $p < 0.01$.

However, compound 3 exhibited concentration-dependent anticancer activities and its IC_{50} values were calculated as 8.19 and 23.41 µM for MCF-7 and MDA-MB-231 cell lines, respectively. The IC_{50} values of other compounds were also given in Table 1. Isatin derivatives with substituent groups (-OCH₃, -F and -Cl) with different sizes and varying electronic properties at the C-5 position have cytotoxicity effects. Isatins including methoxy group (1-4) have better cytotoxicity activity than fluoro (5) and chloro (6) on the isatins against MCF-7 cells. When the methoxy group is known as the electron-donating group, the fluoro and chloro atoms are electron-withdrawing kind. Therefore, the electron-donating methoxy group connected to the C-5 position is beneficial to the activity, while the electron-withdrawing fluorine and chlorine are harmful to the activity. When comparing compounds 5 and 6, compound 5 was higher activity than compound 6 due to fluoro atoms had better electronegative atoms or strong electron-withdrawing groups than chloro atoms.

Table 1. The IC₅₀ values of the molecules **1-6** in MCF-7 and MDA-MB-231 cell lines. The cells were exposed to various concentrations of purposed structures between 5 to 80 μM, and the cytotoxicity was evaluated using the XTT assay.

Compounds	R ₁ /R ₂	Inhibition of cell growth (IC ₅₀ , μM)	
		MCF-7	MDA-MB-231
1	CH ₃ /5-OCH ₃	18.14	> 80
2	C ₂ H ₅ /5-OCH ₃	19.81	> 80
3	CH ₂ CH=CH ₂ /5-OCH ₃	8.19	23.41
4	3-OCH ₃ C ₆ H ₄ /5-OCH ₃	21.42	> 80
5	3-ClC ₆ H ₄ /5-F	22.67	> 80
6	2-FC ₆ H ₄ /5-Cl	41.16	> 80
Standard	Cisplatin	27.9	33.7

Metabolic enzymes inhibition results

hCA I and II isoenzymes inhibition results

There is a broad variety of pharmacological uses for inhibition of these isoforms with many classes of CA inhibitor (CAI) compounds, beginning with anti-glaucoma and diuretic agents, anti-obesity, anti-epileptics, or anti-tumor drugs, and ending with anti-arthritis and anti-neuropathic anti-ischemic pain drugs. Indeed, this is only possible since different hCA isozymes are involved in very different pathologies of the 16 reported to date [43]. The findings shown in Table 2 and Figure 1 indicate that the thiosemicarbazone derivatives with isatin (**1-6**) have an effective inhibition profile against slow cytosolic isoform hCA I. The hCA I isoform was inhibited at low nanomolar levels by these compounds (**1-6**), with K_i varying from 2.01 ± 0.35 to 21.55 ± 2.56 μM. On the other hand, because of its widespread inhibition of CAs, acetazolamide (AZA), known to be a broad-specific CA inhibitor, showed a K_i value of 37.04 ± 5.47 μM against hCA I. Outstanding hCA I inhibitors with K_i of 2.01 ± 0.35 and 3.21 ± 0.45 μM were obtained from the **6** and **5** inhibitors, respectively. The hCA I inhibition effects of thiosemicarbazone derivatives including isatin (**1-6**) were found to be greater than that of a clinically normal CA inhibitor, acetazolamide. For hCA I, AZA's IC₅₀ values as positive regulation and some combinations of thiosemicarbazone derivatives (**1-6**), the following order: **6** (1.57 μM, r²: 0.9661) < **5** (2.05 μM, r²: 0.9913) < **4** (6.02 μM, r²: 0.9593) < **1** (9.35 μM, r²: 0.9725) < **AZA** (35.42 μM, r²: 0.9262). Against the physiologically dominant isoform hCA II, these compounds (**1-6**) demonstrated K_is varying from 1.24±0.33 to 25.03±5.48 μM (Table 2). These compounds (**1-6**) were observed to have high inhibition effects on hCA II. On the other hand, standard compound AZA showed K_i of 34.55 ± 4.36 μM against hCA II. The **6** and **5** had shown the most inhibition effect with K_i values of 1.24 ± 0.33 and 3.98 ± 0.52 μM, respectively. For hCA II, IC₅₀ values of AZA as positive control and some compounds synthesized in this study; the following order: **6** (1.04 μM, r²: 0.9790) < **5** (3.11 μM, r²: 0.9586) < **4** (4.35 μM, r²: 0.9932) < **1** (6.47 μM, r²: 0.9937) < **AZA** (28.37 μM, r²: 0.9454). In the prevention of altitude sickness and glaucoma treatment, the potent CA inhibitors AZA and methazolamide have been widely used clinically as weak diuretic causes.

AChE inhibition results

Recently researchers have shown a lot of interest in the recording of AChE inhibitors. In addition, it is also said that selective AChE inhibitors can avoid classical cholinergic toxicity [44]. The development of new selective AChE inhibitor compounds may also provide additional benefits in the treatment of AD. Recently, the extension of selective AChE inhibitors has been of significant interest. The AChE inhibitory activity of thiosemicarbazone derivatives with isatin (**1-6**) was significantly higher than that of normal AChE inhibitors such as Tacrine. The K_i values for these

compounds (**1-6**) and regular compound (tacrine) are further summarized in Table 2. As can be seen from the results obtained in Table 2, these compounds (**1-6**) effectively inhibited AChE, with K_i values in the range of 40.37 ± 8.23 to 125.43 ± 24.93 μM . However, all these compounds (**1-6**) had almost similar inhibition profiles. The most active **5** showed K_i values of 40.37 ± 8.23 μM . For AChE, IC_{50} values of TAC as positive control and some novel compounds were studied in this study the following order: **5** (48.37 μM , r^2 : 0.9812) < **2** (92.36 μM , r^2 : 0.9527) < **6** (98.33 μM , r^2 : 0.9437) < TAC (108.20 μM , r^2 : 0.9767).

Table 2. The enzyme inhibition results of the compounds (**1-6**) against human carbonic anhydrase isoenzymes I and II (hCA I and II), acetylcholinesterase (AChE) and α -glycosidase (α -Gly) enzymes

Compd.	IC_{50} (μM)								K_i (μM)			
	hCA I	r^2	hCA II	r^2	AChE	r^2	α -Gly	r^2	hCA I	hCA II	AChE	α -Gly
1	9.35	0.9725	6.47	0.9937	104.37	0.9924	993.26	0.9612	12.52 ± 2.14	8.43 ± 0.94	83.27 ± 14.84	1056.47 ± 56.07
2	15.48	0.9741	12.57	0.9408	92.36	0.9527	1025.37	0.9632	18.31 ± 3.04	15.47 ± 2.30	72.36 ± 7.35	1003.75 ± 111.63
3	17.45	0.9889	22.54	0.9883	154.38	0.9487	495.37	0.9305	21.55 ± 2.56	25.03 ± 5.48	125.43 ± 24.93	564.35 ± 72.06
4	6.02	0.9593	4.35	0.9932	111.25	0.9489	734.05	0.9698	7.98 ± 0.97	6.12 ± 1.04	93.46 ± 13.44	683.437 ± 66.58
5	2.05	0.9913	3.11	0.9586	48.37	0.9812	692.11	0.9824	3.21 ± 0.45	3.98 ± 0.52	40.37 ± 8.23	722.38 ± 91.26
6	1.57	0.9661	1.04	0.9790	98.33	0.9437	620.38	0.9629	2.01 ± 0.35	1.24 ± 0.33	82.22 ± 13.08	594.38 ± 52.04
AZA*	35.42	0.9262	28.37	0.9454	-	-	-	-	37.04 ± 5.47	34.55 ± 4.36	-	-
TAC**	-	-	-	-	108.20	0.9767	-	-	-	-	67.05 ± 23.64	-
ACR***	-	-	-	-	-	-	511.94	0.9462	-	-	-	645.44 ± 71.04

*Acetazolamide (AZA) was used as a control for hCA I and II. **Tacrine (TAC) was used as a control for AChE enzyme. ***Acarbose (ACR) was used as a control for α -glycosidase enzyme.

α -Glycosidase inhibition results

Several alpha-glucosidase inhibitors have recently been identified and tested. Anti-diabetic medications such as acarbose, voglibose, and miglitol, which are used in clinical practice, competitively suppress alpha-glucosidase in the brush boundary of the small intestine, thus interrupting carbohydrate hydrolysis and enhancing postprandial hyperglycemia. For enzyme glycosidase, thiosemicarbazone derivatives including isatin (**1-6**) have IC_{50} values in the range of $495.37 - 1025.37$ μM and K_i in the range of $564.35 \pm 72.06 - 1056.47 \pm 56.07$ μM (Table 2). The results have documented that all these compounds (**1-6**) have shown the inhibitory effects of α -glycosidase similar to acarbose (IC_{50} : 511.94 μM) as a standard glycosidase inhibitor. The most effective K_i values of **3** and **6** were with K_i values of 564.35 ± 72.06 and 594.38 ± 52.04 μM , respectively. For α -glycosidase, IC_{50} values of ACR as positive control and some compounds (**1-6**) the following order: **3** (495.37 μM , r^2 : 0.9305) < ACR (511.94 μM) < **6** (620.38 μM , r^2 : 0.9629) < **5** (692.11 μM , r^2 : 0.9824). Diabetes management currently includes the administration of oral hypoglycemic agents such as biguanide, thiazolidinedione, sulphonylurea, and alpha-glucosidase inhibitors, among others.

Molecular docking studies

Pharmacokinetics properties of all compounds were determined to understand their drug-likeness properties and the properties have been presented in Table 3. The compounds were compatible with Lipinski's rule [45-47] due to molecular weight, hydrogen bond acceptor/donor, and octanol/water partition coefficient. They exhibit great cell membrane permeability with Caco and MDCK values and have good oral absorption properties. They also are non-toxic and don't block the Human ether-a-go-go-related gene (hERG) potassium channels, due to rtvFG and LogHERG values, respectively. As a result, the compounds can be accepted as a drug their good drug-likeness properties.

Table 3. Pharmaceutically properties of thiosemicarbazone derivatives including isatin.

Comp.	^a rtvFG	^b MW	^c DHB	^d AHB	^e logPo/w	^f logHERG	^g Caco	^h logBB	ⁱ PMDCCK	^j % Hum. oral abs.
1	0	264.30	2.00	5.75	1.51	-4.65	583.01	-0.67	609.29	85.34
2	0	278.32	2.00	5.75	1.90	-4.91	667.09	-0.73	665.59	88.67
3	0	290.33	2.00	5.75	2.20	-5.25	655.17	-0.82	653.03	90.24
4	0	356.39	2.00	5.75	3.05	-6.08	730.82	-0.84	703.76	96.11
5	0	348.78	2.00	5.00	3.47	-5.99	797.46	-0.36	3219.7	100.0
6	0	348.78	2.00	5.00	3.49	-6.09	728.96	-0.40	1327.7	100.0

^aReactive group (tox), ^bMolecular weight, ^cNumber of hydrogen bond donors, ^dNumber of hydrogen bond acceptors, ^eOctanol/water partition coefficient, ^fIC₅₀ value for blockage of HERG K⁺ channels, ^gCaco-2 cell membran permeability, ^hBrain/blood partition coefficient, ⁱMDCK Cell permeability in nm/sec, ^jQualitative human oral absorption.

Catalytic active sites of the enzymes were identified by analysing the crystal structures. The sites have 1.063, 0.971, 1.090, and 1.016 of Sitescore. The scores have shown that all predicted binding sites can be accepted as a catalytic active sites. The sites were used for the evaluation of best-posed docking hits. Following catalytic active site detection, the induced-fit docking method was validated by the re-docking co-crystallized ligand of each enzyme, and co-crystallized and re-docked ligand positions were illustrated in Figure 3. The ligands have located in very close positions with 0.446 Å, 0.452 Å, 0.106 Å, and 0.450 Å. The RMSD values have indicated that the docking method was very reliable for analyzing possible inhibition mechanisms.

The most active thiosemicarbazone derivatives with isatin was docked with co-crystallized ligands in the same way, and their binding affinity was calculated. In the negative direction, the posture with the highest binding affinity score was selected as the best posture, and the binding affinity of the compound in the best posture was listed in Table 4.

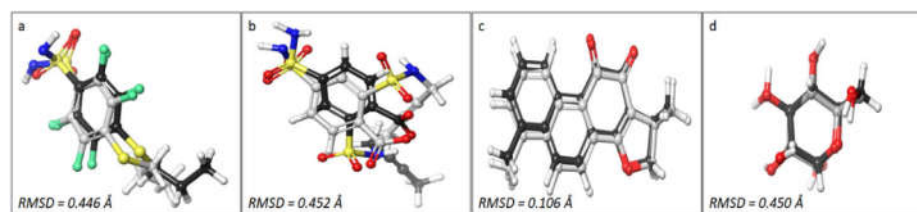


Figure 3. Induced-fit docking method validation. a) 2,3,5,6-tetrafluoro-4-(propylsulfanyl) benzenesulfonamide, b) 2-(but-2-yn-1-ylsulfamoyl)-4-sulfamoyl benzoic acid, c) dihydrotanshinone I, and d) D-glucose.

The findings revealed that compounds **5** and **6** exhibited well binding affinity against hCA II and AChE, respectively in comparison to their standard inhibitors. Also, their binding modes were analyzed for detection of their possible inhibition mechanism. Compound **6** is well located in the catalytic active site of hCA I enzyme via 5-chloro-2-oxoindolin-3-ylidene and hydrazine-1-

carbothioamide moieties (Figure 4a-left). Same moieties constituted interaction with active site residues. 5-chloro-2-oxoindolin-3-ylidene moiety formed an aromatic hydrogen bond with Gln92. The chlorobenzene ring was surrounded by 200-207 residues (Figure 4). The most important interactions for enzyme inhibition were constituted between the moiety and His67 as seen in Figure 4a-right. The Trp5, His67, and His200 are located at the entrance of the active-site channel [48]. The interactions between compound **6** and the residues may block entering the substrate.

Table 4. The binding affinity score (kcal/mol) of the most active thiosemicarbazone derivatives including isatin among the enzyme catalytic sites.

Compounds	Docking score			
	hCA I	hCA II	AChE	α -Glucosidase
3	-	-	-	-4.946
5	-	-	-9.932	-
6	-6.697	-8.251	-	-
AZA*	-9.016	-9.560	-	-
TAC**	-	-	9.579	-
ACR***	-	-	-	-16.933

*Acetazolamide (AZA) was used as a standard inhibitor for human carbonic anhydrase isoenzymes I, and II (hCA I, and II). **Tacrine (TAC) was used as a standard inhibitor for acetylcholinesterase (AChE) enzyme. ***Acarbose (ACR) was used as a standard inhibitor for α -glycosidase enzyme taken from reference.

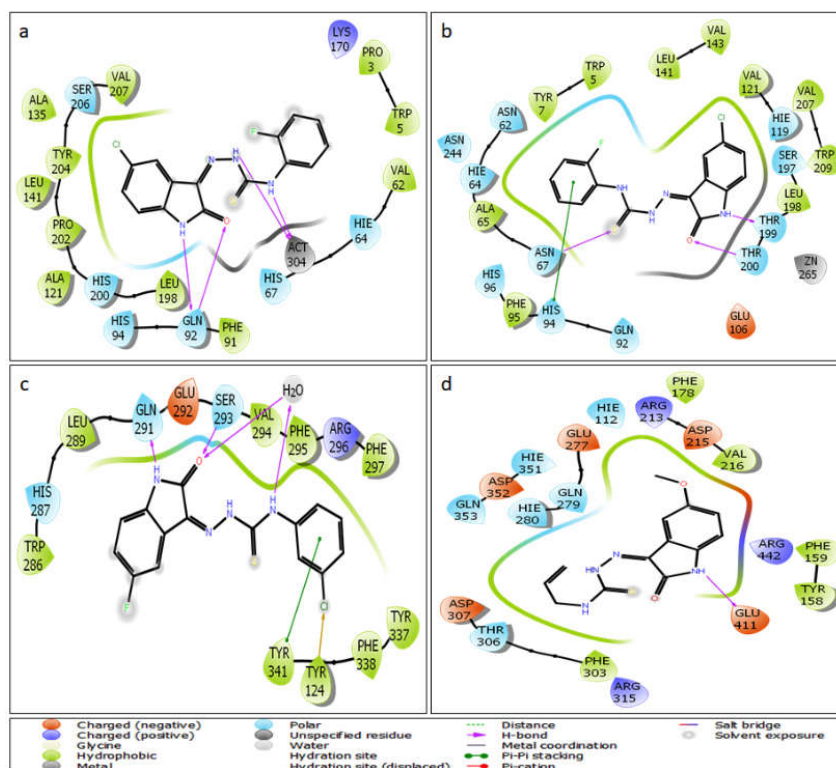


Figure 4. 2D interaction mode between compounds and enzymes a) **6**-hCA I, b) **6**-hCA II, c) **5**-AChE, and d) **3**- α -glucosidase.

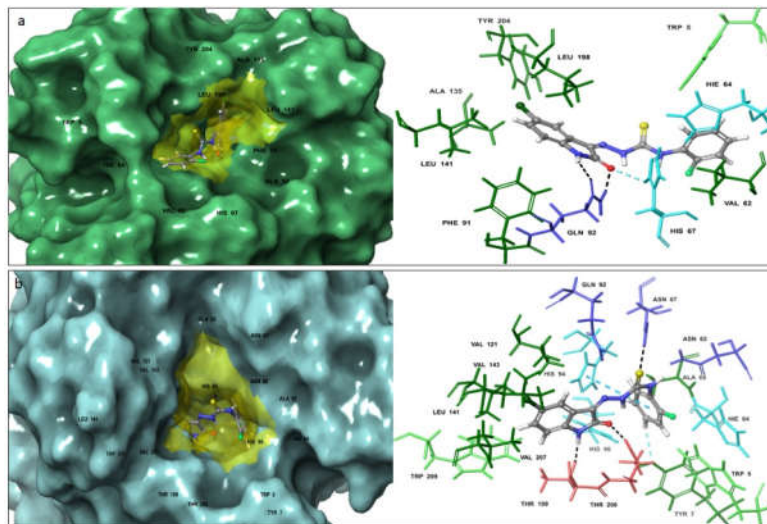


Figure 5. Detailed interaction mode of compound **6**. a) **6**-hCA I and b) **6**-hCA II. The position of compounds in the catalytic active sites has presented on the left side. 3D detailed binding mode of compounds have presented on the right side. The compounds have presented as grey ball-stick model, amino acids have presented as residue type colored thick-tube model. Catalytic active sites have presented as yellow solid surfaces.

In addition, compound **6** was the most active compound against hCA II enzyme. Hydrazine-1-carbothioamide moiety formed a hydrogen bond with Asn67. Ivanova *et al.* [49] have indicated that 1-*N*-alkylated-6-sulfamoyl saccharin derivatives inhibited hCAII enzyme by interacting Asn67 and Gln92. The hydrophobic region (Val121, Val143 and Leu198) accommodated the chlorobenzene ring of compound **6** and flor phenyl ring formed π - π stacking interaction with His94. 5-chloro-2-oxoindolin-3-ylidene moiety formed hydrogen bonds with Thr198 and Thr200. The two residues are key residues for enzyme catalytic activity because they contribute its activity by interacting with zinc-bonded water molecules in the catalytic active site (Ivanova *et al* 2015). As a result, compound **6** inhibits hCA II enzyme interacting with key residues for catalytic activity as shown in Figure 5.

5-Fluoro-2-oxoindolin-3-ylidene moiety of compound **5** embedded in deep active site gorge as seen in Figure 6a-left, and it formed hydrogen bonds with Gln291 and Ser293 (Figure 4c). Besides, hydrazine-1-carbothioamide moiety formed a water-mediated hydrogen bond with Ser293 (Figure 6a-right). Many AChE inhibitors lead to irreversible inhibition of the enzyme through covalent modification of Ser293 [50]. For this reason, interactions between compound **5** and Ser293 were critical for enzyme inhibition. Additionally, its chlorophenyl ring interacted with Tyr124 and Tyr431 through halogen bond and π - π stacking interaction, respectively. The interactions that formed with peripheral site residues contributed to enzyme inhibition. Compound **3** has a low binding affinity against α -glucosidase. Because it has formed a hydrogen bond with Asp441 via 5-methoxy-2-oxoindolin-3-ylidene moiety as seen in Figure 4d. The aromatic ring of the moiety also formed an aromatic hydrogen bond with the same residue (Figure 6b). The compound is well located in the catalytic active site and it blocked interactions between substrate and catalytic active site residues.

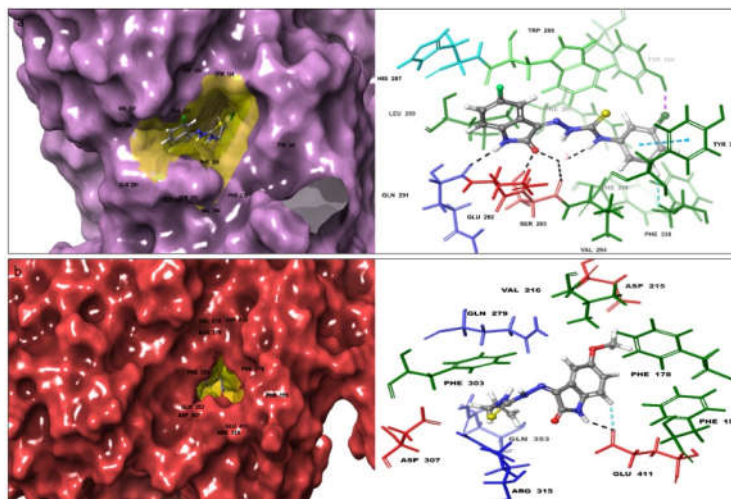


Figure 6. Detailed interaction mode of compounds. a) 5-AChE, and b) 3- α -glucosidase. The position of compounds in the catalytic active sites has presented on the left side. 3D detailed binding mode of compounds have presented on the right side. The compounds have presented as grey ball-stick model, amino acids have presented as residue type colored thick-tube model. Catalytic active sites have presented as yellow solid surfaces.

CONCLUSION

Isatin-based thiosemicarbazone derivatives were investigated. The 2-oxoindolin-3-ylidene moiety of each compound has contributed to the inhibition of hCA I, hCA II, and AChE enzymes by interfering with the catalytic active site residues of each enzyme. However, it didn't contribute to the inhibition of the α -glucosidase enzyme. Furthermore, the aromatic rings in the compounds have been key factors in the inhibition of these enzymes through interactions with hydrophobic residues. When compared to their standard inhibitors, compounds **5** and **6** showed a high binding affinity for hCA II and AChE, respectively. Furthermore, cytotoxicity data demonstrated compound **3** to be more effective against both MCF-7 and MDA-MB-231 cell lines.

ACKNOWLEDGMENTS

This work was supported by Scientific Research Project Fund of Sivas Cumhuriyet University (Project number SHMYO-013). The authors acknowledge the financial support through Researchers Supporting Project number (RSP2023R147), King Saud University, Riyadh, Saudi Arabia.

REFERENCES

1. Ferlay, J.; Soerjomataram, I.; Dikshit, R.; Eser, S.; Mathers, C.; Rebelo, M.; Parkin, D.M.; Forman, D.; Bray, F. Cancer incidence and mortality worldwide: sources, methods and major patterns in GLOBOCAN 2012. *Int. J. Cancer* **2015**, *136*, E359–E386.
2. Emami, S.; Dadashpour, S. Current developments of coumarin-based anti-cancer agents in medicinal chemistry. *Eur. J. Med. Chem.* **2015**, *102*, 611–630.

3. Wan, Y.; Fang, G.; Chen, H.; Deng, X.; Tang, Z. Sulfonamide derivatives as potential anti-cancer agents and their SARs elucidation. *Eur. J. Med. Chem.* **2021**, *226*, 113837.
4. Xu, M.; Peng, Y.; Zhu, L.; Wang, S.; Ji, J.; Rakesh, K.P. Triazole derivatives as inhibitors of Alzheimer's disease: current developments and structure-activity relationships. *Eur. J. Med. Chem.* **2019**, *180*, 656–672.
5. Hargreaves, R.J. “It Ain't over'til It's over” a-The search for treatments and cures for Alzheimer's disease. *ACS Med. Chem. Lett.* **2012**, *3*, 862–866.
6. Palmer, A.M. Neuroprotective therapeutics for Alzheimer's disease: progress and prospects. *Trends Pharmacol. Sci.* **2011**, *32*, 141–147.
7. Kumar, B.; Kumar, V.; Prashar, V.; Saini, S.; Dwivedi, A.R.; Bajaj, B.; Mehta, D.; Parkash, J.; Kumar, V. Dipropargyl substituted diphenylpyrimidines as dual inhibitors of monoamine oxidase and acetylcholinesterase. *Eur. J. Med. Chem.* **2019**, *177*, 221–234.
8. Güzel E.; Koçyiğit, Ü.M.; Taslimi, P.; Erkan, S.; Taskin, O.S. Biologically active phthalocyanine metal complexes: Preparation, evaluation of α -glycosidase and anticholinesterase enzyme inhibition activities, and molecular docking studies. *J. Biochem. Mol. Toxicol.* **2021**, *35*, 1–9.
9. Rahman, M.S.; Uddin, M.S.; Rahman, M.A.; Samsuzzaman, M.; Behl, T.; Hafeez, A.; Perveen, A.; Barreto, G.E.; Ashraf, G.M. Exploring the role of monoamine oxidase activity in aging and alzheimer's disease. *Curr. Pharm. Des.* **2021**, *27*, 4017–4029.
10. Ismail, M.M.; Kamel, M.M.; Mohamed, L.W.; Faggal, S.I. Synthesis of new indole derivatives structurally related to donepezil and their biological evaluation as acetylcholinesterase inhibitors. *Molecules* **2012**, *17*, 4811–4823.
11. O'Bryant, S. E.; Gupta, V.; Henriksen, K.; Edwards, M.; Jeromin, A.; Lista, S.; Bazenet, C.; Soares, H.; Lovestone, S.; Hampel, H.; Montine, T.; Blennow, K.; Foroud, T.; Carrillo, M.; Graff-Radford, N.; Laske, C.; Breteler, M.; Shaw, L.; Trojanowski, J.Q.; Schupf, N.; Martins, R. Guidelines for the standardization of preanalytic variables for blood-based biomarker studies in Alzheimer's disease research. *Alzheimer's & Dementia* **2015**, *11*(5), 549–560.
12. Lahiri, D.K.; Farlow, M.R.; Greig, N.H.; Sambamurti, K. Current drug targets for Alzheimer's disease treatment. *Drug Dev. Res.* **2002**, *56*, 267–281.
13. Kumar, R.S.; Almansour, A.I.; Arumugam, N.; Althomili, D.M.Q.; Altaf, M.; Basiri, A.; Kotresha, D.; Manohar, T.S.; Venketesh, S. Ionic liquid-enabled synthesis, cholinesterase inhibitory activity, and molecular docking study of highly functionalized tetrasubstituted pyrrolidines. *Bioorg. Chem.* **2018**, *77*, 263–268.
14. Imtaiyaz, H.M.; Shajee, B.; Waheed, A.; Ahmad, F.; Sly, W.S. Structure, function and applications of carbonic anhydrase isozymes. *Bioorg. Med. Chem.* **2013**, *21*, 1570–1582.
15. Swietach, P.; Hulikova, A.; Vaughan-Jones, R.D.; Harris, A.L. New insights into the physiological role of carbonic anhydrase IX in tumour pH regulation. *Oncogene* **2010**, *29*, 6509–6521.
16. Swietach, P.; Vaughan-Jones, R.D.; Harris, A.L. Regulation of tumor pH and the role of carbonic anhydrase 9. *Cancer Metastasis Rev.* **2007**, *26*, 299–310.
17. Koçyiğit, Ü.M.; Taslimi, P.; Tüzün, B.; Yakan, H.; Muğlu, H.; Güzel, E. 1, 2, 3-Triazole substituted phthalocyanine metal complexes as potential inhibitors for anticholinesterase and antidiabetic enzymes with molecular docking studies. *J. Biopl. Struct. Dyn.* **2022**, *40*, 4429–4439.
18. Rana, S.; Blowers E.C.; Tebbe, C.; Contreras, J.I.; Radhakrishnan, P.; Kizhake, S.; Zhou, T.; Rajule, R.N.; Arnst, J.L.; Munkarah, A.R.; Rattan, R.; Natarajan, A. Isatin derived spirocyclic analogues with α -methylene- γ -butyrolactone as anticancer agents: A structure–activity relationship study. *J. Med. Chem.* **2016**, *59*, 5121–5127.
19. Pape, V.F.S.; Tóth, S.; Füredi, A.; Szebényi, K.; Lovrics, A.; Szabó, P.; Wiese, M.; Szakács, G. Design, synthesis and biological evaluation of thiosemicarbazones,

- hydrazinobenzothiazoles and arylhydrazones as anticancer agents with a potential to overcome multidrug resistance. *Eur. J. Med. Chem.* **2016**, 117, 335–354.
20. Premanathan, M.; Radhakrishnan, S.; Kulangiappar, K. Antioxidant & anticancer activities of isatin (1H-indole-2, 3-dione), isolated from the flowers of *Couroupita guianensis* Aubl. *Indian J. Med. Res.* **2012**, 136, 822–826.
 21. Yakan, H.; Serdar, Ç.M.; Kurt, B.Z.; Muğlu, H.; Sönmez, F.; Güzel, E. A new series of asymmetric bis-isatin derivatives containing urea/thiourea moiety: Preparation, spectroscopic elucidation, antioxidant properties and theoretical calculations. *J. Mol. Struct.* **2021**, 1239, 130495.
 22. Meleddu, R.; Distinto, S.; Corona, A.; Bianco, G.; Cannas, V.; Esposito, F.; Artese, A.; Alcaro, S.; Matyus, P.; Bogdan, D.; Cottiglia, F.; Tramontano, E.; Maccioni, E. (3Z)-3-(2-[4-(aryl)-1, 3-thiazol-2-yl] hydrazin-1-ylidene)-2, 3-dihydro-1H-indol-2-one derivatives as dual inhibitors of HIV-1 reverse transcriptase. *Eur. J. Med. Chem.* **2015**, 93, 452–460.
 23. Akdemir, A.; Güzel-Akdemir, Ö.; Karali, N.; Supuran, C.T. Isatin analogs as novel inhibitors of *Candida* spp. β -carbonic anhydrase enzymes. *Bioorg. Med. Chem.* **2016**, 24, 1648–1652.
 24. Sahoo, S.; Mahendrakumar, C.B.; Setty, C.M. Synthesis, antiinflammatory and antibacterial activities of some substituted isatin and isatin fused with 3-substituted 4-amino-5-mercapto-1,2,4-triazoles. *Int. J. Chem. Sci.* **2015**, 13, 613–624.
 25. Ibrahim, H.S.; Abou-Seri, S.M.; Tanc, M.; Elaasser, M.M.; Abdel-Aziz, H.A.; Supuran, C.T. Isatin-pyrazole benzenesulfonamide hybrids potently inhibit tumor-associated carbonic anhydrase isoforms IX and XII. *Eur. J. Med. Chem.* **2015**, 103, 583–593.
 26. Havrylyuk, D.; Zimenkovsky, B.; Vasylenko, O.; Gzella, A.; Lesyk, R. Synthesis of new 4-thiazolidinone-, pyrazoline-, and isatin-based conjugates with promising antitumor activity. *J. Med. Chem.* **2012**, 55, 8630–8641.
 27. Melis, C.; Meleddu, R.; Angeli, A.; Distinto, S.; Bianco, G.; Capasso, C.; Cottiglia, F.; Angius, R.; Supuran, C.T.; Maccioni, E. Isatin: a privileged scaffold for the design of carbonic anhydrase inhibitors. *J. Enzyme Inhib. Med. Chem.* **2017**, 32, 68–73.
 28. Eldehna, W.M.; Fares, M.; Ceruso, M.; Ghabbour, H.A.; Abou-Seri, S.M.; Abdel-Aziz, H.A.; El Ella, D.A.A.; Supuran, C.T. Amido/ureidosubstituted benzenesulfonamides-isatin conjugates as low nanomolar/subnanomolar inhibitors of the tumor-associated carbonic anhydrase isoform XII. *Eur. J. Med. Chem.* **2016**, 110, 259–266.
 29. Muğlu, H. Synthesis, characterization, and antioxidant activity of some new N 4-arylsubstituted-5-methoxyisatin- β -thiosemicarbazone derivatives. *Res. Chem. Intermed.* **2020**, 46, 2083–2098.
 30. Stanojkovic, T.P.; Kovala-Demertzi, D.; Primikyri, A.; Garcia-Santos, I.; Castineiras, A.; Juranic, Z.; Demertzis, M.A. Zinc (II) complexes of 2-acetyl pyridine 1-(4-fluorophenyl)-piperazinyl thiosemicarbazone: Synthesis, spectroscopic study and crystal structures–Potential anticancer drugs. *J. Inorg. Biochem.* **2010**, 104, 467–476.
 31. Yakan, H.; Koçyiğit, Ü.M.; Muğlu, H.; Ergul, M.; Erkan, S.; Güzel, E.; Taslimi, P.; Gülçin, İ. Potential thiosemicarbazone-based enzyme inhibitors: Assessment of antiproliferative activity, metabolic enzyme inhibition properties, and molecular docking calculations. *J. Biochem. Mol. Toxicol.* **2022**, 36, e23018.
 32. Nepali, K.; Sharma, S.; Sharma, M.; Bedi, P.M.S.; Dhar, K.L. Rational approaches, design strategies, structure activity relationship and mechanistic insights for anticancer hybrids. *Eur. J. Med. Chem.* **2014**, 77, 422–487.
 33. Güzel, E.; Yarasir, M.N.; Özkaya, A.R. Low symmetry solitaire-and trans-functional porphyrazine/phthalocyanine hybrid complexes: Synthesis, isolation, characterization, and electrochemical and in-situ spectroelectrochemical properties. *Synth. Met.* **2020**, 262, 116331.
 34. Ding, Z.; Zhou, M.; Zeng, C. Recent advances in isatin hybrids as potential anticancer agents. *Arch. Pharm.* **2020**, 353, 1900367.

35. Ahmad, M.; Pervez, H.; Zaib, S.; Yaqub, M.; Naseer, M.M.; Khan, S.U.; Iqbal, J. Synthesis, biological evaluation and docking studies of some novel isatin-3-hydrazone-thiazolines. *RSC Adv.* **2016**, *6*, 60826–60844.
36. Tao, Y.; Zhang, Y.; Cheng, Y.; Wang, Y. Rapid screening and identification of α -glucosidase inhibitors from mulberry leaves using enzyme-immobilized magnetic beads coupled with HPLC/MS and NMR. *Biomed. Chromatogr.* **2013**, *27*, 148–155.
37. Verpoorte, J.A.; Mehta, S.; Edsall, J.T. Esterase activities of human carbonic anhydrases B and C. *J. Biol. Chem.* **1967**, *242*, 4221–4229.
38. Ellman, G.L.; Courtney, K.D.; Andres, V.; Featherstone, R.M. A new and rapid colorimetric determination of acetylcholinesterase activity. *Biochem. Pharmacol.* **1961**, *7*, 88–95.
39. Ishaq, M.; Taslimi, P.; Shafiq, Z.; Khan, S.; Ekhteiari Salmas, R.; Zangeneh, M.M.; Saeed, A.; Zangeneh, A.; Sadeghian, N.; Asari, A.; Mohamad, H. Synthesis, bioactivity and binding energy calculations of novel 3-ethoxysalicylaldehyde based thiosemicarbazone derivatives. *Bioorg. Chem.* **2020**, *100*, 103924.
40. Karimov, A.; Orujova, A.; Taslimi, P.; Sadeghian, N.; Mammadov, B.; Karaman, H.S.; Farzaliyev, V.; Sujayev, A.; Tas, R.; Alwasel, S.; Gulçin, İ. Novel functionally substituted esters based on sodium diethyldithiocarbamate derivatives: Synthesis, characterization, biological activity and molecular docking studies. *Bioorg. Chem.* **2020**, *99*, 103762.
41. Božić, A.R.; Filipovic, N.; Novakovic, I.; Bjelogrić, S.; Nikolić, J.B.; Drmanić, S.Z.; Marinković, A.D. Synthesis, antioxidant and antimicrobial activity of carbohydrazones. *J. Serbian Chem. Soc.* **2017**, *82*, 495–508.
42. Yakan, H. Preparation, structure elucidation, and antioxidant activity of new bis (thiosemicarbazone) derivatives. *Turk. J. Chem.* **2020**, *44*, 1085–1099.
43. Lipinski, C.; Lombardo, F.; Dominy, B.W.; Feeney, P.J. Experimental and computational approaches to estimate solubility and permeability in drug discovery and development settings. *Adv. Drug Deliv. Rev.* **1997**, *46*, 3–25.
44. Nocentini, A.; Lucidi, A.; Perut, F.; Massa, A.; Tomaselli, D.; Gratteri, P.; Baldini, N.; Rotili, D.; Mai, A.; Supuran, C.T. α , γ -Diketocarboxylic acids and their esters act as carbonic anhydrase IX and XII selective inhibitors. *ACS Med. Chem. Lett.* **2019**, *10*, 661–665.
45. Derosa, G.; Maffioli, P. α -Glucosidase inhibitors and their use in clinical practice. *Arch. Med. Sci.* **2012**, *8*, 899.
46. Waziri, I.; Wahab, O.O.; Mala, G.A.; Oselusi, S.O.; Egieyeh, S.A.; Nasir, H. Zinc(II) complex of (Z)-4-((4-nitrophenyl)amino)pent-3-en-2-one, a potential antimicrobial agent: Synthesis, characterization, antimicrobial screening, DFT calculation and docking study. *Bull. Chem. Soc. Ethiop.* **2023**, *37*, 633–651.
47. Abou-Melha, K. Synthesis, characterization, biological activity, molecular docking and thermal analysis of binuclear complexes. *Bull. Chem. Soc. Ethiop.* **2022**, *36*, 843–858.
48. Alterio, V.; Monti, S.M.; Truppo, E.; Pedone, C.; Supuran, C.T.; De Simone, G. The first example of a significant active site conformational rearrangement in a carbonic anhydrase-inhibitor adduct: the carbonic anhydrase I–topiramate complex. *Org. Biomol. Chem.* **2010**, *8*, 3528–3533.
49. Ivanova, J.; Leitans, J.; Tanc, M.; Kazaks, A.; Zalubovskis, R.; Supuran, C.T.; Tars, K. X-ray crystallography-promoted drug design of carbonic anhydrase inhibitors. *Chem. Commun.* **2015**, *51*, 7108–7111.
50. Cheung, J.; Gary, E.N.; Shiomi, K.; Rosenberry, T.L. Structures of human acetylcholinesterase bound to dihydrotanshinone I and territrem B show peripheral site flexibility. *ACS Med. Chem. Lett.* **2013**, *4*, 1091–1096.